Non-orthogonal stress modes for interfacial fracture based on local plastic dissipation

Jae Hyun Kim [*]

Department of Mechanical Engineering, ME3053, Korea Advanced Institute of Science and Technology, 373-1, Kusung-Dong, Yusung-Gu, Daejeon 305-701, South Korea

Abstract

Interfacial cracks have several features which are different from those of cracks in homogeneous materials. Among those, the loading mode dependency of interfacial toughness has been a main obstacle to the widespread utilization of interfacial fracture mechanics. In this study, plasticity-induced toughening of an interface crack between an elastic–plastic material and an elastic material is studied. A useful relationship between the plastic dissipation and the plastic zone size is derived via an effective crack length model. Non-orthogonal stress modes for interface cracks are proposed on the basis of the plastic dissipation mechanism and a mixed-mode criterion for interfacial crack growth is also proposed using these stress modes. The non-orthogonal stress modes are able to represent the asymmetric behavior, mode-dependent toughening and ε-dependency of interfacial crack growth.
© 2002 Elsevier Science Ltd. All rights reserved.

Keywords: Plastic dissipation; Interfacial fracture mechanics; Toughness; Mode dependency; Effective crack length

1. Introduction

Many modern material systems consist of more than two materials. Defined as a boundary between two dissimilar materials, interfaces are essential geometries for these material systems. In most cases, the interface is a very weak geometry depending on the manufacturing processes. Furthermore, the reliability of the material systems is largely affected by the behavior of the interface. Following the successful application of fracture mechanics to a crack in a homogeneous material, interfacial fracture mechanics has been considered as a promising tool for evaluating the reliability of multi-material systems. Applying the interfacial fracture mechanics to practical reliability problems includes the following steps: the finite element (FE) modeling of real structures, the measurement of interfacial toughness for the specific material combinations and the comparison of the crack driving force with the toughness data. However, there are several obstacles to the wide adoption of the interfacial fracture mechanics: (i) the local loading phase angle does

[*] Tel.: +82-42-869-3053; fax: +82-42-869-3210.

E-mail address: skms@kaist.ac.kr (J.H. Kim).

not coincide with the external loading; (ii) the local loading phase angle is not constant along the interface; (iii) the interfacial toughness is dependent on the loading phase angle; and (iv) it is hard to measure and characterize the interfacial fracture toughness over a wide range of mode mixity. Via FE modeling and the conservation integral method [1], (i) can be solved. To solve (ii)–(iv), an appropriate definition of the characteristic length and an accurate model for interfacial toughening mechanisms are required.

Many researchers have studied the behavior of interfacial cracks. Williams [2] determined the elastic stress singularity of the interface crack. Rice and Sih [3], Park and Earmme [4], Hutchinson and Suo [5] among others presented solutions of useful problems. With the increasing importance of plastic behavior, some researchers [6–10] analyzed the elastic–plastic behavior of interface cracks. Experimental works by a number of workers [11–17] revealed that interfacial toughness is strongly dependent on loading mode and that plastic dissipation can be a major mechanism for this dependency. Tvergaard and Hutchinson [18] presented the plasticity-induced toughening behavior of an interfacial crack between an elastic–plastic material and a rigid material using the method of Needleman [19]. The main issue in the mode dependency of interfacial toughness is to separate the plastic dissipation energy from the total dissipation energy [20–22]. To calculate the plastic dissipation during crack growth, the local fracture process must be taken into account as well as the material's local plastic behavior. Tvergaard and Hutchinson's method embedding the local separation law seems powerful for calculating the plastic dissipation energy during crack growth. But their method requires high computation-cost and several undetermined parameters in the present status. In a practical sense, the undetermined parameters can be regarded as curve fitting parameters.

The objective of this study is to model the plasticity-induced toughening mechanism during interfacial crack growth and to propose a useful framework of interfacial fracture mechanics based on the plastic dissipation mechanism. A useful relationship between the plastic dissipation and the plastic zone size is derived via an effective crack length model. Two non-orthogonal stress modes are proposed to represent the asymmetric behavior of interfacial crack growth. A quite simple and accurate criterion for mixed-mode interfacial toughness is proposed using the non-orthogonal stress modes. The formal framework of the interfacial fracture mechanics is discussed in terms of non-orthogonal stress modes and the effect of the bimaterial constant ε is emphasized in the case of interfacial crack growth accompanying plastic dissipation.

In what follows, we begin with an effective crack length model in order to derive a relationship between plastic dissipation and plastic zone size. Then a numerical scheme to evaluate the plastic zone size is described. The formal framework of interfacial fracture mechanics is presented with the help of non-orthogonal stress modes. Application to experimental results is presented to reveal the usefulness of the proposed theory. Finally, discussion and summary are described.

2. Effective crack length model for plastic dissipation

Plastic dissipation energy during crack growth is estimated using an effective crack length model. The effective crack length is the summation of physical crack length (a) and plastic zone correction crack length (a_p). Plastic deformation around the crack tip is approximated via the plastic zone correction crack length as described in Appendix A. In order to estimate the plastic dissipation energy during crack growth, fracture process within local plastic zone must be taken into account. However, modeling of the fracture process is very expensive and time consuming even in simplified problems [18]. In the present model, specifying the change of the plastic zone correction crack length during fracture process substitutes for the modeling of the local fracture process. A similar model for a crack in a homogeneous material can be found in Shivakumar and Crew's [23] work.

Consider a specimen with a crack lying along the interface between two dissimilar, isotropic solids as shown in Fig. 1. The upper solid (#1) is an elastic–plastic material characterized by μ_1, v_1, σ_{YS}, n, α, and deforms under uniaxial tension according to the Ramberg–Osgood relation $\varepsilon = \sigma/E + \alpha(\sigma/\sigma_{YS})^n$. The
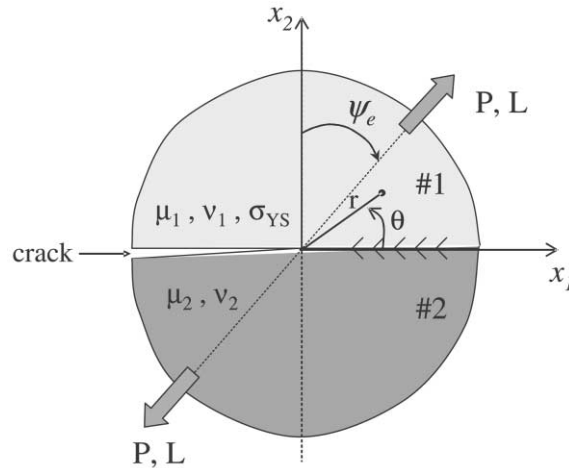
Fig. 1. Geometry of a bimaterial specimen with an interface crack.

lower solid (#2) is an elastic material with μ_2 and v_2. Since most bimaterial systems have weak interfaces, it is assumed that crack extension occurs along the interface. It is also assumed that plastic zone size around the interfacial crack is much smaller than crack length (small scale yielding condition). The external loading and displacement parameters are P, ψ_e and L as shown in Fig. 1. A schematic of load–displacement curve for this specimen is displayed in Fig. 2. The non-linear behavior in the curve is due to the elastic–plastic behavior of material #1 (The non-linear region is greatly exaggerated for clarity). We choose a displacement-controlled fracture test for convenience although a similar argument can be applied to a load-controlled test.

During crack extension Δa, the total dissipation energy is represented by area BCFE, which is the summation of surface generation energy (area BCD) and plastic dissipation energy (area CFED) (see Fig. 2). Using some approximations and algebraic manipulations, we obtain the surface generation, the plastic dissipation and the total dissipation energies as (detailed derivation is described in Appendix B):

$$E_{\text{surface}} = 2\gamma_{12}\Delta a, \tag{1}$$

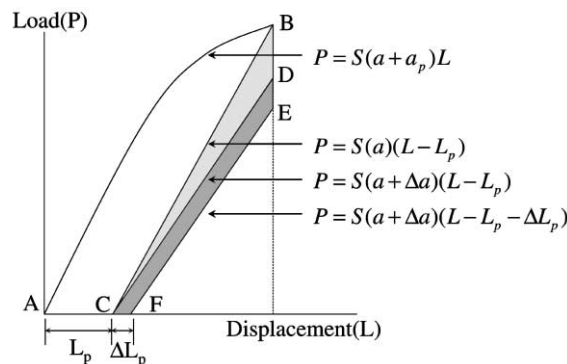$$E_{\text{plastic}} = 4\gamma_{12}C_1 r_y \Delta a, \tag{2}$$

Fig. 2. Surface generation (triangle CDB) and plastic dissipation (rectangle CDEF) energies in a schematic of load–displacement curve.

$$E_{\text{total}} = 2\gamma_{12}\{1 + 2C_1 r_y\}\Delta a, \tag{3}$$

where γ_{12} is the surface energy per unit area between material #1 and #2, r_y is the plastic zone length along the interface (i.e. plastic zone size in the direction of crack extension), and C_1 is a material constant accounting for plastic dissipation behavior of an interface. This simple relationship between plastic dissipation and plastic zone length agrees well with our intuition that the plastic dissipation increases with the increase of the plastic zone size. However, other alternative measures of plastic zone size should be compared with the plastic zone length r_y and the relationship given by Eq. (2) or (3) should be verified using a rigorous numerical simulation embedding a local fracture process model. These are discussed in Section 6.

Note that since the plastic zone length along the interface r_y can be determined from specimen geometry, loading conditions, boundary conditions and material properties, the only parameters to characterize interfacial crack growth under mixed-mode loading are γ_{12} and C_1. The parameters γ_{12} and C_1 must be determined from experimental results. In the next section, we estimate r_y using an approximate method and present useful results on the qualitative behavior of r_y.

3. Numerical scheme for evaluating plastic zone size (elastic approximation of elastic–plastic behavior)

In the previous section, we derive a relationship between plastic dissipation energy and plastic zone length. Now we proceed to evaluate the plastic zone size around the interfacial crack tip using an elastic approximation. Zywicz and Parks [24] used the same procedures to evaluate the plastic zone size and showed that the overall size and the shape of the plastic zone are well characterized by the elastic approximation. As the strain-hardening exponent decreases, the elastic approximation becomes more precise.

Consider a crack lying along the interface between two isotropic solids with material #1 above and material #2 below (refer to Fig. 1). Material #1 is an elastic–plastic material characterized by μ_1, v_1, σ_{YS} and a strain-hardening exponent n, while material #2 is a linearly elastic material characterized by μ_2 and v_2. When the strain-hardening exponent n approaches 1, we can estimate the plastic zone size approximately as following. The crack lies on the plane $x_2 = 0$ with $x_1 < 0$ and traction vanishes on the crack surfaces. Plane strain condition is assumed. The asymptotic stress fields for the interface crack are given by

$$\sigma_{\alpha\beta} = \frac{K}{\sqrt{2\pi r}}(\cos(\psi + \varepsilon\ln(r/h))\Sigma_{\alpha\beta}^{\text{I}}(\theta) + \sin(\psi + \varepsilon\ln(r/h))\Sigma_{\alpha\beta}^{\text{II}}(\theta)), \quad (\alpha, \beta = 1, 2). \tag{4}$$

Here h is the characteristic length, the real stress intensity factor K is defined as $(\sigma_{22} + i\sigma_{12})|_{\theta=0} = Ke^{i\psi}(r/h)^{i\varepsilon}/\sqrt{2\pi r}$, and the angular functions $\Sigma_{\alpha\beta}(\theta)$ of superscripts I and II are presented in Rice et al.'s [25] work. The bimaterial constant ε under plane strain condition is given by

$$\varepsilon = \frac{1}{2\pi}\ln\left[\frac{(3 - 4v_1)/\mu_1 + 1/\mu_2}{1/\mu_1 + (3 - 4v_2)/\mu_2}\right]. \tag{5}$$

Using Eq. (4), Mises equivalent stress ($\bar{\sigma}_M$) in solid #1 can be obtained. Equating the Mises equivalent stress $\bar{\sigma}_M$ with yield strength σ_{YS} of material #1 yields the elastic–plastic boundary around the interface crack in material #1. The elastic–plastic boundary estimated by the elastic approximation is dependent on the loading phase angle ψ, bimaterial constant ε, and Poisson's ratio of material #1, v_1 while the actual elastic–plastic boundary is dependent on the hardening exponent n and α, as well as ψ, ε, and v_1. The dependency on v_1 disappears under plane stress. Zywicz and Parks [24] showed that the elastic approximation overestimates the plastic zone size behind the crack tip and underestimates it ahead of the crack tip as the strain-hardening exponent increases. They also showed that the elastic approximation well represents the overall plastic zone shape and converges to the actual elastic–plastic behavior when the hardening
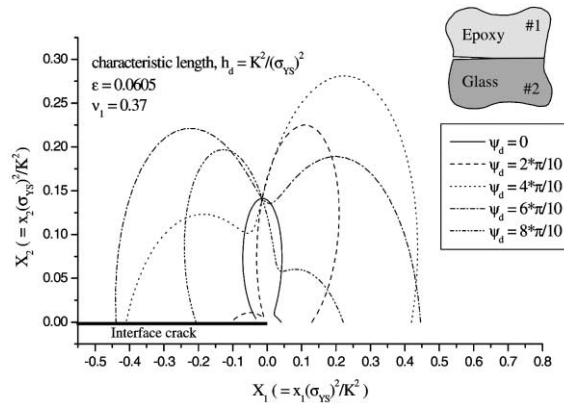
Fig. 3. Plastic zone shapes around an interface crack between epoxy and glass.

exponent decreases. Fig. 3 shows an elastic approximation of the elastic–plastic boundary for an interfacial crack between epoxy and glass with various loading phase angles.

The previous section shows that the plastic dissipation is proportional to the size of the plastic zone along the line $\theta = 0$ (the distance from the crack tip to the elastic–plastic boundary in the direction of crack extension). The normalized plastic zone length $r_y \sigma_{YS}^2 / K^2$ is shown in Fig. 4. In Fig. 4, the loading phase angle ψ denotes a ratio of shear stress and normal stress at a characteristic length $h = K^2 / \sigma_{YS}^2$. It is found that a minimum plastic zone length is located around $\psi = 0$, but the precise location of the minimum is dependent on bimaterial constant ε. When $\varepsilon = 0$ (non-oscillatory material case), conventional mode I loading ($\psi = 0$) leads to a minimum plastic zone length and conventional mode II loading ($\psi = \pi/2$) leads to a maximum plastic zone length. As ε deviates from 0, the local loading phase angle for minimum and maximum plastic zone lengths deviates from 0 and $\pi/2$, respectively. As shown in the previous section, the minimum plastic zone length corresponds to the minimum plastic dissipation and vice versa under the pre-mentioned conditions. In order to characterize the total dissipation energy using Eq. (3), the plastic zone length must be determined together with the two parameters C_1 and γ_{12}. Although it is possible to calculate the plastic zone length under given loading and geometric conditions, the functional form of the plastic zone length is not easy to handle as shown in Fig. 4 and depends on the material properties ε and v_1 as well
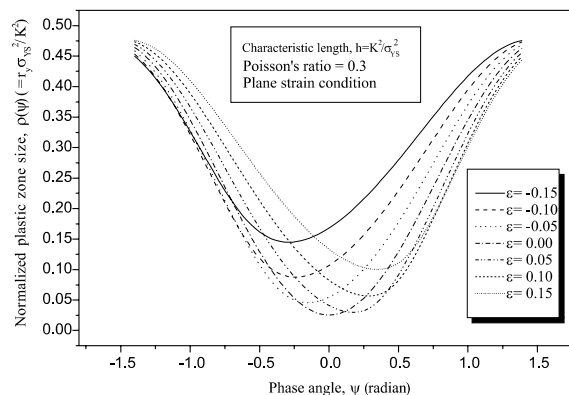

Fig. 4. Normalized plastic zone length as a function of phase angle.

as the plastic properties of material #1. In the next section, we propose two non-orthogonal stress modes to estimate the plastic dissipation more simply and a two-parameter model of interfacial toughness to represent the behavior of interfacial crack growth under various loading phase angles.

4. Formal framework of interfacial fracture mechanics

In Section 3 it is shown that the plastic dissipation is dependent on the local loading phase angle ψ for a given material combination (given ε), and the local loading phase angle at which the minimum or maximum plastic dissipation occurs varies with the material combination. In this section, we propose a new definition for the characteristic length h and the loading mode based on the plastic dissipation mechanism (a useful discussion of characteristic length can be found in Rice's [26] work).

The minimum plastic dissipation mode is defined as c-mode (crack driving mode) and the maximum plastic dissipation mode is defined as p-mode (plastic dissipation mode). In order to be consistent with the non-oscillatory material case ($\varepsilon = 0$), the characteristic length is selected so that the c-mode corresponds to $\psi = 0$. $\psi = 0$ refers to the mode I loading (crack tip opening mode) in the non-oscillatory material case. The characteristic length can be written as

$$h = \lambda \frac{K^2}{\sigma_{\text{YS}}^2},$$

(6)

where λ is a non-dimensional length parameter and is determined from when the plastic zone length has a minimum at the loading mode $\psi = 0$ as follows.

The Mises equivalent stress $\overline{\sigma}_{\text{M}}$ around the interface crack tip is expressed as

$$\overline{\sigma}_{\text{M}} = \frac{K}{\sqrt{2\pi r}} M(\psi + \varepsilon \ln(r/h), \theta, \varepsilon, v_1),$$

(7)

where $M(\psi + \varepsilon \ln(r/h), \theta, \varepsilon, v_1)$ can be calculated from the angular functions $\Sigma_{\alpha\beta}^{\text{I}}$ and $\Sigma_{\alpha\beta}^{\text{II}}$ of Eq. (4) (Zywicz and Parks [24] presented the simple form of Mises equivalent stress). Poisson's ratio of material #1, v_1 is included under plane strain, but is not needed under plane stress. Since the elastic–plastic boundary is defined by $\overline{\sigma}_{\text{M}} = \sigma_{\text{YS}}$, the plastic zone length along the interface ($\theta = 0$) is a root of

$$\frac{K}{\sqrt{2\pi r}} M(\psi + \varepsilon \ln(r/h), 0, \varepsilon, v) = \sigma_{\text{YS}}.$$

(8)

Using the non-dimensional radius, $\rho = r\sigma_{\text{YS}}^2/K^2$ and Eq. (6), Eq. (8) is given by

$$\frac{1}{\sqrt{2\pi\rho}} M(\psi + \varepsilon \ln(\rho/\lambda), 0, \varepsilon, v) = 1.$$

(9)

A non-dimensional length parameter λ is selected so that the non-dimensional plastic zone length along the interface has a minimum at $\psi = 0$. The phase difference ξ between c- and p-mode is determined so that the non-dimensional plastic zone length along the interface has a maximum at $\psi = \xi$, where ψ is associated with the characteristic length $h = \lambda K^2/\sigma_{\text{YS}}^2$. In oscillatory material systems, the phase difference ξ is not $\pi/2$ while the phase difference between modes I and II in non-oscillatory material systems is $\pi/2$. This can explain the asymmetric toughening in interfacial fracture data. Since the phase difference between c- and p-mode is not $\pi/2$ in oscillatory bimaterial systems, plastic dissipation behavior is not symmetric with respect to the line $\psi = 0$ (minimum plastic dissipation mode or minimum toughness mode). When ξ is greater than $\pi/2$, the plasticity-induced toughening in positive ψ grows more slowly than the toughening in negative ψ. When ξ is less than $\pi/2$, the converse is true. The parameters λ and ξ are only dependent on ε and v_1 as shown in Fig. 5(a) and (b). Note that the parameters λ and ξ are determined from the elastic approximation
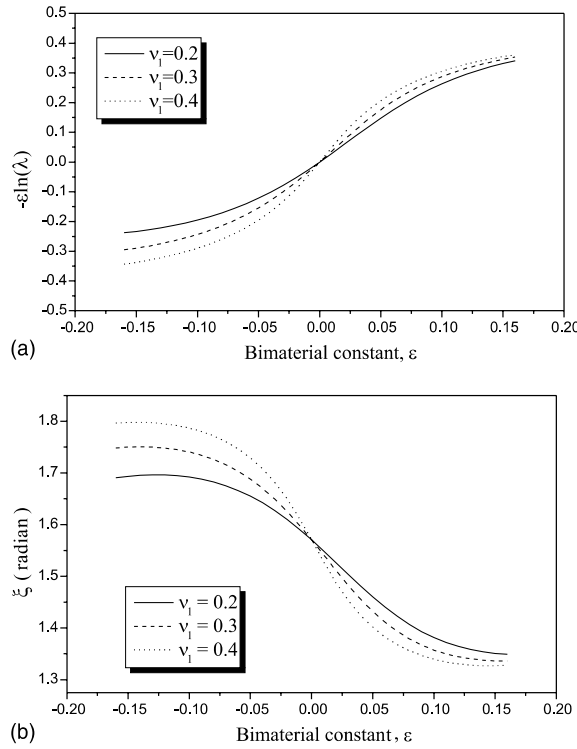
Fig. 5. (a) Non-dimensional length parameter and (b) phase difference between minimum and maximum plastic dissipation modes.

for the elastic–plastic behavior. The elastic approximation seems sufficient to characterize the overall behavior of the plastic zone as mentioned in Section 3, but if a more precise calculation is desired, FE analysis embedding the real elastic–plastic behavior of material #1 can be used (comparison with a rigorous FE analysis is given in Section 6). In this study only the elastic approximation is used to determine the parameters λ and ξ. The formal representation of interfacial fracture mechanics can be given by means of the c- and p-modes as following.

Consider an interfacial crack between two dissimilar materials, with material #1 above and material #2 below under small scale yielding. Material #1 is an elastic–plastic material characterized by E_1, v_1, σ_{YS}, α, n and deforms under uniaxial tension according to the Ramberg–Osgood relation $\varepsilon = \sigma/E + \alpha(\sigma/\sigma_{YS})^n$. Since small scaling yielding is assumed, a dominant elastic K field exists and the plastic zone is very small compared to crack length and the size of the elastic K field. The interface crack tip stress field is fully characterized by bimaterial constant ε, stress intensity K and loading phase angle ψ associated with the characteristic length h as given by Eq. (4). All interfacial crack stress fields can be decomposed into c- and p-mode as shown in Fig. 6. The c-mode stress field accompanies the minimum plastic dissipation when the crack extends while the p-mode stress field accompanies the maximum plastic dissipation during the crack extension. Using the c-mode and the p-mode stress intensity factors, K_c and K_p all given interfacial stress fields can be written by

$$\sigma_{22} + \mathrm{i}\sigma_{12}\big|_{\theta=0} = \frac{K}{\sqrt{2\pi r}} \mathrm{e}^{\mathrm{i}\psi} \left(\frac{r}{\lambda K^2/\sigma_{YS}^2} \right)^{\mathrm{i}\varepsilon} = \frac{K_c}{\sqrt{2\pi r}} \left(\frac{r}{\lambda K_c^2/\sigma_{YS}^2} \right)^{\mathrm{i}\varepsilon} + \frac{K_p}{\sqrt{2\pi r}} \mathrm{e}^{\mathrm{i}\xi} \left(\frac{r}{\lambda K_p^2/\sigma_{YS}^2} \right)^{\mathrm{i}\varepsilon}. \tag{10}$$
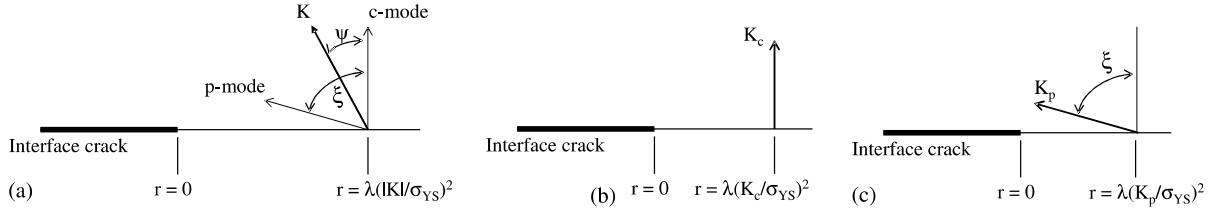
Fig. 6. Separation of modes: (a) applied K-field can be decomposed into (b) c-mode K-field and (c) p-mode K-field.

The unique relations among K_c, K_p, ξ, K and ψ are given by

$$\begin{cases} \cos(\psi) = x\cos(-\varepsilon\ln x^2) + y\cos(\xi - \varepsilon\ln y^2), \\ \sin(\psi) = x\sin(-\varepsilon\ln x^2) + y\sin(\xi - \varepsilon\ln y^2), \end{cases} \tag{11}$$

where $x = K_c/K$ and $y = K_p/K$. We can obtain a simpler relation under $(x \ll y)$ or $(y \ll x)$ or $(y \approx x$ and $|\varepsilon| \ll 1)$ as

$$\begin{cases} \cos(\psi) = x + y\cos(\xi), \\ \sin(\psi) = y\sin(\xi). \end{cases} \tag{12}$$

The elastic energy release rate for crack extension along the interface is given by

$$G = \frac{K^2}{H} = \frac{1}{H}\left\{ \left(K_c + K_p\cos(\xi)\right)^2 + \left(K_p\sin(\xi)\right)^2 \right\}. \tag{13}$$

Using c-mode fracture toughness K_{cf}, a mixed-mode fracture criterion is expressed as

$$\left[K_c + qK_P\cos(\xi)\right]^2 + \left[qK_P\sin(\xi)\right]^2 = K_{cf}^2, \tag{14}$$

where q is a ratio of c-mode toughness to p-mode toughness. Since the p-mode stress state accompanies maximum plastic dissipation during crack extension, the p-mode toughness is always larger than the c-mode toughness. In other words, q is always <1. For an ideally brittle interface which does not accompany plastic dissipation during crack extension, q equals 1. Eq. (14) can be written in the form of energy release rate as

$$\Gamma(\psi) = \frac{G_f}{\{-\sin(\psi - \xi)/\sin(\xi) + q\sin(\psi)/\tan(\xi)\}^2 + \{q\sin(\psi)\}^2}, \tag{15}$$

where $G_f = K_{cf}^2/H$ and ψ is the local loading phase angle associated with the characteristic length $h = \lambda K^2/\sigma_{YS}^2$. Similar forms of interfacial fracture criteria can be found in Hutchinson and Suo's [5] work as

$$\Gamma(\psi) = \frac{G_f}{1 + (\omega - 1)\sin^2\psi}, \tag{16}$$

$$\Gamma(\psi) = G_f[1 + (1 - \omega)\tan^2\psi], \tag{17}$$

where ω is a fitting parameter similar with q. Eqs. (16) and (17) are two-parameter criteria for non-oscillatory materials. But since these criteria assume that the toughness has a minimum at $\psi = 0$, these criteria should be modified in oscillatory bimaterials as

$$\Gamma(\psi) = \frac{G_f}{1 + (\omega - 1)\sin^2(\psi - \psi_o)}, \tag{18}$$

$$\Gamma(\psi) = G_f[1 + (1 - \omega)\tan^2(\psi - \psi_o)], \tag{19}$$

where ψ_o is a phase shift. These are three-parameter models [27]. G_f, ω and ψ_o must be determined from experimental data. Charalambides et al. [28] proposed a similar model with three parameters. However, the model proposed in this study requires only two parameters to represent the toughness data of an oscillatory material combination, and the asymmetric behavior of interfacial fracture toughness due to plasticity is included in the model.

5. Application to experimental data

We present here an example to show the usefulness of the proposed interfacial fracture model. Since Liechti and Chai's interfacial toughness data are measured with high precision and a wide range of load phase angle, we select their data as the example. Their specimen was an edge-cracked bimaterial strip made of glass and epoxy, and tested under displacement-controlled conditions. The specimen geometry has an expression for energy release rate independent of crack length a. The bimaterial constant ε of the specimen and the Poisson's ratio of epoxy are 0.0605 and 0.37, respectively. With this value, we can obtain the non-dimensional length parameter λ and the phase difference ξ between c- and p-mode as $\lambda = 0.0239$ and $\xi = 1.39$ (79.6°), respectively, from Fig. 5(a) and (b). The fact that the loading phase angle difference (ξ) between the minimum plastic dissipation mode and the maximum plastic dissipation mode is not $\pi/2$ (90°) indicates asymmetric toughening behavior of the specimen. For example, a loading of positive phase angle $\pi/3$ (60°) gives a different plastic dissipation from that of negative phase angle $-\pi/3$ ($-60°$).

We use the characteristic length $h = \lambda K^2/\sigma_{YS}^2$, while in the original paper $h_o = 12.7$ mm (the yield strength of epoxy, σ_{YS} is 40.4 MPa). The phase angle ψ_o in the original paper can be readily transformed via the simple formula:

$$\psi = \psi_o + \varepsilon \ln(h/h_o). \tag{20}$$

We can then represent their experimental data with the proposed mixed-mode interfacial toughness criterion, Eq. (14). We find that the pair of $q = 0.02$ and $K_{cf} = 136000$ Pa (m)$^{1/2}$ gives the best fit of the toughness data, as shown Fig. 7. Fig. 7 shows that the asymmetric toughening effect is included in this toughness criterion and a very close fit with the experimental data can be obtained with only two parameters. Note that the phase difference ξ is not a fitting parameter but a pre-calculated one using the elastic approximation of the elastic–plastic behavior of the materials. We can observe that a minimum
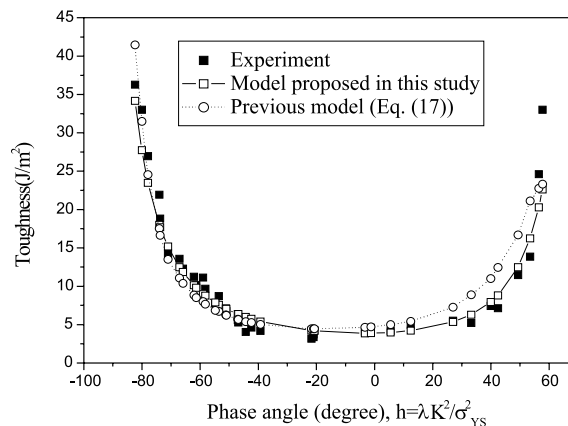

Fig. 7. Comparison of toughness models with experimental data [14].

Table 1
Interfacial fracture parameters for some bimaterials [13]

Bimaterial	α	β	ε	λ	ξ	G_f (N/m)	q
Aluminum/epoxy	0.90	0.218	−0.071	0.0473	1.735	24.0	0.57
Brass/epoxy	0.94	0.228	−0.074	0.0495	1.738	10.0	0.34
Steel/epoxy	0.96	0.232	−0.075	0.0503	1.739	7.1	0.059
Plexiglass/epoxy	−0.15	−0.029	0.009	0.0159	1.540	34.0	0.49

Epoxy: shear modulus—1.5 GPa, Poisson's ratio—0.34, yield strength—85 MPa.

toughness occurs at the c-mode ($\psi = 0$). Since other criteria, Eqs. (18) and (19), cannot include the asymmetric behavior of toughness, the least square fits of experimental data using these criteria show poor coincidence with the data in spite of requiring three parameters.

Following the above procedures, we can represent any experimental toughness data with good accuracy. Table 1 shows the curve fitting results of some bimaterials' toughness data (these are Wang and Suo's [13] data). Note that only G_f and q in Table 1 are fitting parameters while the other parameters are determined from material's elastic properties. Since the proposed fracture criterion equation (15) has two parameters and includes the plastic dissipation mechanism, we can characterize the mode-dependent interfacial toughness by conducting two fracture tests which give different phase angles from each other.

6. Discussion

We propose a model for plasticity-induced toughening of an interfacial crack in the proceeding sections. Although it presents some useful results, verifications and further discussions are required because it relies on several assumptions and a simplified numerical scheme. We discuss the relationship between plastic dissipation and plastic zone length, alternative methods for determining c- and p-mode, toughness model and the non-orthogonal stress modes.

6.1. Relationship between plastic dissipation and plastic zone length

In Section 2, we arrive at the simple relationship between the plastic dissipation and the plastic zone length as expressed by Eq. (2). This relationship implies that the plastic dissipation is linearly proportional to the plastic zone length, and the total dissipation energy is the linear scaling of the plastic zone length (see Eq. (3)). Since this relationship contains several assumptions, it requires verification. In this subsection, we compare this relationship with rigorous numerical calculations by Tvergaard and Hutchinson [18]. They analyzed an interface crack between an elastic–plastic solid and a rigid solid under small scale yielding, and embedded a local fracture process model (i.e. cohesive zone model) in their FE model. They dealt with a single material combination $\varepsilon = 0.0813$. Their calculation must be carefully interpreted because of differences in their numerical model and the present model. In their model, the work of fracture Γ_o is taken as crack initiation toughness, but in our model the initiation toughness is taken as the summation of surface generation energy $2\gamma_{12}$ and plastic dissipation energy. Since Γ_o has a different physical meaning from the surface generation energy $2\gamma_{12}$, the plastic dissipation energy cannot be directly obtained by means of subtracting Γ_o from their toughness results.

Using the method mentioned in Section 3, we calculate normalized plastic zone length $\rho_y = r_y \sigma_{YS}^2 / K_o^2$ as a function of ψ_o, where ψ_o is measured with $h_o = (1/3\pi)K_o^2/\sigma_{YS}^2$ (K_o is a stress intensity factor corresponding to Γ_o and is defined by Eq. (3.9) in Tvergaard and Hutchinson's [18] work). Fig. 8 shows that the
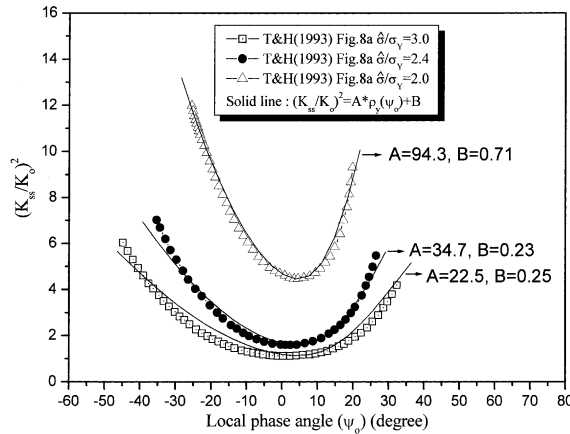
Fig. 8. Comparison of the proposed relationship (Eq. (3)) with numerical results by Tvergaard and Hutchinson [18].

linear scaling of the normalized plastic zone length well represents the toughness results in Tvergaard and Hutchinson's [18] work. This verifies the relationship expressed by Eq. (2) or (3).

6.2. Alternative methods for determining c- and p-modes

The c- and p-modes are defined as minimum and maximum plastic dissipation modes, respectively. It is difficult to calculate the plastic dissipation energy rigorously because it requires a local fracture process model. Thus, we determine the c- and p-modes using the plastic zone length (the relationship between the plastic dissipation and the plastic zone length is derived via the effective crack length model in Section 2). However, there may be alternative methods for determining the c- and p-modes. One alternative method can be devised using height of plastic zone. Another method can be devised using volume of plastic zone.

In this subsection, we compare three alternative methods for determining c- and p-modes with rigorous numerical results by Tvergaard and Hutchinson [18]. We choose three parameters for determining c- and p-modes as plastic zone length, plastic zone height and volume of plastic zone. The plastic zone length r_y is a distance from a crack tip to the elastic–plastic boundary along the interface as mentioned in Section 2. The plastic zone height, r_h is defined as a distance from a crack tip to the elastic–plastic boundary along the line $\theta = \pi/2$. The volume of plastic zone, V_p is defined as $2r_y r_h$ (for a unit thickness of plastic zone). All three parameters are calculated using the procedure described in Section 3, and compared with the toughness curve in Tvergaard and Hutchinson's [18] work. Other curves in Tvergaard and Hutchinson's [18] work give similar results. Fig. 9 shows comparison of these three parameters with the toughness curve. Although r_y and $2r_y r_h$ curves show a similar trend to phase angle, the plastic zone length r_y gives the best representation of the toughness curve, and the local phase angle of minimum toughness coincides that of minimum plastic zone length. This feature justifies the use of the plastic zone length in determining the c-mode (minimum plastic dissipation or toughness mode) and the p-mode (maximum plastic dissipation or toughness mode). Note that maximum toughness data is required to justify the p-mode determination strictly, but it was not obtained in Tvergaard and Hutchinson's [18] work.

6.3. Toughness model

In Section 4, a toughness model is proposed based on non-orthogonal stress modes and simplified energy balance argument. Although the model gives an accurate fit of Liechti and Chai's data, it has a minimum
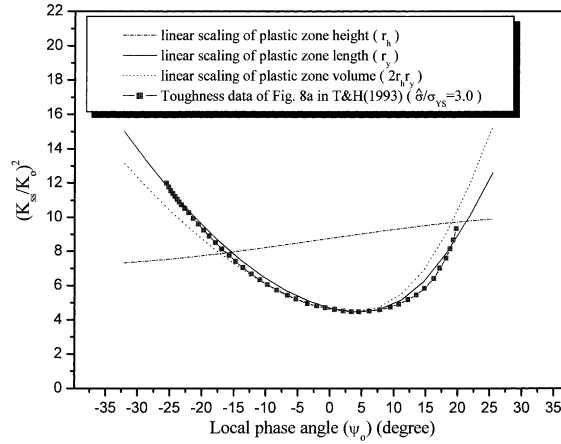
Fig. 9. Comparison of numerical results [18] with three alternative methods for determining c- and p-modes.

toughness at the phase angle that slightly deviates from $\psi = 0$ (in most cases, this deviation is negligibly small). This feature is not consistent with our assertion that the stress mode of minimum toughness corresponds to $\psi = 0$. Other phenomenological models for interfacial toughness can be given based on the non-orthogonal stress modes. One alternative model is written by

$$\Gamma(\psi) = \begin{cases} \dfrac{G_c}{\cos^2(\psi\pi/2\xi) + q^2\sin^2(\psi\pi/2\xi)} & \psi \geqslant 0, \\[3mm] \dfrac{G_c}{\cos^2(\psi\pi/2(\xi-\pi)) + q^2\sin^2(\psi\pi/2(\xi-\pi))} & \psi < 0, \end{cases} \tag{21}$$

where ψ is measured with the characteristic length $h = \lambda(K/\sigma_{YS})^2$. While phase angle difference between modes I and II is $\pi/2$ for a crack in a homogeneous material, the phase angle difference between c- and p-mode is ξ (not $\pi/2$) for an interface crack in an oscillatory bimaterial. Thus, the phase angle range of $-\pi/2 < \psi < \pi/2$ for a crack in a homogeneous material must be transformed into $\xi - \pi < \psi < \xi$ for an interface crack. Minimum plastic dissipation mode corresponds to $\psi = 0$ for both a crack in a homogeneous material and an interface crack in a bimaterial. Maximum plastic dissipation modes for a crack in a homogeneous material or a bimaterial with $\varepsilon = 0$ are $\psi = \pi/2$ and $\psi = -\pi/2$; and a symmetrical toughness curve with respect to the line $\psi = 0$ is obtained. However, for an interface crack ($\varepsilon \neq 0$) the maximum plastic dissipation modes are $\psi = \xi$ and $\psi = \xi - \pi$; and an asymmetrical toughness curve with respect to the line $\psi = 0$ is obtained.

6.4. Non-orthogonal stress modes and framework of fracture mechanics

In this study, two independent stress modes, c- and p-mode, are defined on the basis of plastic dissipation behavior and are not orthogonal to each other. This definition is valid for material combinations of which the interfacial toughness is strongly dependent on the plastic dissipation. If there are other mechanisms that influence the interfacial toughness, appropriate stress modes can be defined based on those mechanisms. The proposed mode definition has the merit that it recovers the conventional crack modes, modes I and II, as the bimaterial constant ε vanishes. Since it contains the conventional stress modes of non-oscillatory material as a special case as well as the interfacial crack stress modes, it is useful for constructing a unified

theory of fracture mechanics including both a crack in a homogeneous material and an interfacial crack in a bimaterial. The unified fracture mechanics will require a unified understanding of crack extension as well as a proper definition of stress modes. The cracks in homogeneous materials tend to kink in the direction of minimizing the mode II stress intensity factor under mixed-mode loading conditions. But for the case of an interfacial crack, the competition among the interfacial toughness and the toughnesses of composing materials must be taken into account to determine the crack growth behavior. The case of $\varepsilon \to 0$ is not identical to the case of a homogeneous material in the sense of crack extension, and the interface of bimaterial systems should be regarded as the third material of the bimaterial systems.

As shown in Fig. 5, the non-orthogonality of stress modes increases with increasing $|\varepsilon|$. If the interfacial crack growth involves no plastic dissipation, any two independent stress modes can be used to predict the behavior of interfacial cracks. Both orthogonal and non-orthogonal stress modes have no effect on the behavior. But for the case of accompanying dominant plastic dissipation together with a large $|\varepsilon|$, the stress mode in the negative phase angle has a much different effect on the interfacial crack from the stress mode in the positive phase angle. Thus the crack growth must be analyzed via the non-orthogonal stress modes. These stress modes result in the asymmetric toughening behavior of the material system. With the non-orthogonal stress modes, it is possible to predict the asymmetric behavior of material systems and the stress mode having the minimum toughness during the interfacial crack growth.

7. Summary

An effective crack length model estimating the plastic dissipation energy is proposed. A useful relationship between the plastic dissipation energy and the plastic zone length is derived using the proposed model. It is shown that the plastic dissipation energy is closely related to the plastic zone length ahead of a crack tip. To present a formal representation of interfacial fracture mechanics, two non-orthogonal, independent stress modes (i.e. c- and p-modes) are introduced on the basis of plastic dissipation. The c- and p-modes converge to the conventional mode I (opening mode) and mode II (shear mode), respectively, as the bimaterial constant ε vanishes. For the case of oscillatory material combinations (ε is not 0), the loading phase angle difference (ξ) between the c-mode and the p-mode is not $\pi/2$; and this non-orthogonality leads to the asymmetric behavior of interfacial toughness. The ε-dependency of the phase angle difference and the non-dimensional characteristic length parameter are clearly estimated by the elastic approximation for the elastic–plastic behavior.

A mixed-mode interfacial toughness criterion is proposed using the c- and p-mode stress intensity factors. The criterion contains only two undetermined parameters, and can include the asymmetric behavior of interfacial fracture toughness and the effects of bimaterial constant, ε. In the case of a bimaterial system having plastic dissipation together with large $|\varepsilon|$. It is critical to use the non-orthogonal stress modes since the non-orthogonality increases as the absolute value of ε increases. As an example, Liechti and Chai's experimental data is analyzed via the proposed criterion. It gives a better fit of experimental data than other criteria in spite of having fewer parameters. It is also emphasized that one can characterize the mode-dependent interfacial toughness by conducting only two fracture tests which give different phase angles from each other.

Using the non-orthogonal stress modes, we can describe the various aspects of an interfacial crack in a simple form, such as asymmetric toughening, ε-dependency, loading phase dependent toughening and the varying plastic zone shape around the crack tip under small scale yielding. It is also shown that a given material combination has a minimum interfacial toughness under the c-mode stress state, which accompanies minimum plastic dissipation. The basic step for the unified framework of fracture mechanics, which combines homogeneous and interfacial fracture mechanics, can be made on the basis of c- and p-mode stress intensity factors.

Acknowledgements

Appendix A. Plastic zone correction crack length

For homogeneous cracks, the effective crack length of Irwin's model is expressed under small scale yielding as

$$a_{\text{eff}} = a + a_{\text{p}} = a + \eta r_y = a + \beta \frac{G\overline{E}}{\sigma_{\text{YS}}^2}, \tag{A.1}$$

where r_y is the plastic zone size ahead of the crack tip, G is the energy release rate, and $\overline{E}$ is $2\mu/(1-v)$ for plane strain condition. η and β are non-dimensional factors which may depend on Poisson's ratio, strain-hardening exponent, etc., but are independent of applied loads and specimen geometries [29,30]. For a perfectly plastic case, $\eta = 1$ and $\beta = 1/(6\pi)$.

For interfacial cracks, a simple model can be made using a similar conceptualization. It is assumed that the interfacial crack propagates along the interface and the plastic zone size is negligibly small compared to crack length (small scale yielding condition). Since the crack lies and propagates along the interface, we estimate the plastic zone size r_y ahead of the crack tip along the interface as shown in Fig. 10. The upper solid (#1) is an elastic–plastic material and the lower solid (#2) is linearly elastic. Once the upper solid yields perfectly plastically, the stiffness of the plastic zone is negligibly small or zero (it can be regarded as the removal of the shaded area in Fig. 10), and the specimen behaves as if the crack extends to the amount of r_y, where r_y corresponds to the plastic zone correction length of the interfacial crack. As the strain-hardening exponent decreases, the plastic zone correction length decreases. When the strain-hardening exponent equals 1 (in this case, the plastic zone has the same modulus as the elastic material), the plastic zone correction length of the interfacial crack reaches zero. In this sense, the effective crack length for the interfacial crack can be expressed as

$$a_{\text{eff}} = a + a_{\text{p}} = a + \eta r_y. \tag{A.2}$$

Under small scale yielding, η is independent of the specimen geometry and applied loads, but may depend on the material properties. r_y is given by

$$r_y = \rho(\psi, \text{material properties}) \frac{GH}{\sigma_{\text{YS}}^2}, \tag{A.3}$$
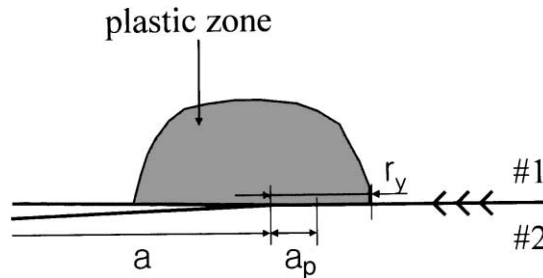

Fig. 10. Effective crack length model for correcting plastic zone around an interface crack.

where ψ is a loading phase angle, G is the elastic energy release rate, $H^{-1} = (1 - \beta^2)(1/\overline{E}_1 + 1/\overline{E}_2)$, and $\overline{E}_i$ is defined as $2\mu_i/(1 - v_i)$ for the plane strain condition. In order to estimate the plastic dissipation energy during the crack growth, it is required that the local fracture process with the local plastic zone should be taken into account. Many researchers have included the fracture process in their analyses using the traction separation law or the cohesive zone model. In the present model, specifying the change of a_p during the fracture process, i.e. $\partial a_p/\partial a$, substitutes for the modeling of the local fracture process.

Appendix B. Derivation of Eqs. (2) and (3)

Consider the load–displacement curve shown in Fig. 2 (for assumptions and applicability range of this argument, refer to Section 2). The load–displacement curve from A to B state can be represented as $P = S(a + a_p)L$ under small scale yielding, where $a_p = \eta r_y$, η is a plastic zone correction factor for an interface crack, r_y is defined as the distance from the interfacial crack tip to the elastic–plastic boundary along the interface, and $S(a + a_p)$ is the elastic stiffness of a specimen with crack length $a + a_p$ (see Appendix A for further discussion). If the specimen is unloaded from B to C state, the load–displacement curve is expressed as $P = S(a)(L - L_p)$. It is noted that the elastic stiffness is not $S(a + a_p)$, but $S(a)$. This is due to the fact that plasticity-induced compliance disappears when the unloading begins. The crack tip dissipation during crack extension can be modeled as the summation of surface generation and plastic dissipation. Surface generation with an amount of Δa results in the load drop from B to D state, and the plastic dissipation corresponding to Δa_p results in the load drop from D to E state. Δa_p is the variation of the plasticity-correction crack length during crack surface generation process, and cannot be fully determined from the conventional plasticity properties. In order to represent the surface generation energy without any plastic dissipation, we cut the interface of the specimen to the amount of Δa and load the specimen as if its materials are linearly elastic. We can then reach D state and the load–displacement curve is written as $P = S(a + \Delta a)(L - L_p)$. At D state, we allow the plastic deformation of the specimen under fixed-displacement; it then experiences a further drop of load and reaches E state. The load at E state is given by

$$P_E = P_D + S'(a + \Delta a)(L - L_p)\Delta a_p = P_D + \{S'(a) + S''(a)\Delta a\}(L - L_p)\Delta a_p$$
$$= P_D + S'(a)(L - L_p)\Delta a_p. \tag{B.1}$$

Again, we unload the specimen from E to F state and the load–displacement curve is expressed as $P = S(a + \Delta a)(L - L_p - \Delta L_p)$. The total dissipation energy in the above procedures is the area BCFE, which is the summation of the surface generation energy (area BCD) and the plastic dissipation energy (area CFED). Thus we can write the following equations:

$$E_{\text{surface}} = (1/2)(L - L_p)(P_B - P_D) = -(1/2)S'(a)(L - L_p)^2\Delta a, \tag{B.2}$$

$$E_{\text{plastic}} = (1/2)(L - L_p)P_D\{1 - (P_E/P_D)^2\} = -(L - L_p)^2 S'(a)\Delta a_p, \tag{B.3}$$

$$E_{\text{total}} = E_{\text{surface}} + E_{\text{plastic}} = -(1/2)S'(a)\{1 + 2(\partial a_p/\partial a)\}(L - L_p)^2\Delta a. \tag{B.4}$$

Since $E_{\text{surface}} = 2\gamma_{12}\Delta a$, where γ_{12} is the surface energy per unit area between material #1 and #2, we can obtain $-(1/2)(L - L_p)^2 S'(a) = 2\gamma_{12}$. Now the plastic dissipation energy and the total dissipation energy are given by

$$E_{\text{plastic}} = 4\gamma_{12}(\partial a_p/\partial a)\Delta a, \tag{B.5}$$

$$E_{\text{total}} = 2\gamma_{12}\{1 + 2(\partial a_p/\partial a)\}\Delta a. \tag{B.6}$$

To calculate the plastic dissipation energy, we must determine the $(\partial a_p / \partial a)|_{L\text{–fixed}}$ term. Since $a_p = \eta r_y$, we can expand $(\partial a_p / \partial a)|_{L\text{–fixed}}$ as

$$(\partial a_p / \partial a)|_{L\text{–fixed}} = \{\partial(\eta r_y)/\partial a\}|_{L\text{–fixed}} = r_y(\partial \eta / \partial a)|_{L\text{–fixed}} + \eta(\partial r_y / \partial a)|_{L\text{–fixed}}. \tag{B.7}$$

The plastic zone length, r_y is proportional to GH/σ_{YS}^2, where G is the elastic energy release rate, H^{-1} is $(1 - \beta^2)(1/\overline{E}_1 + 1/\overline{E}_2)$, and $\overline{E}_i$ is defined as $2\mu_i/(1 - v_i)$ under plane strain. $(\partial r_y / \partial a)|_{L\text{–fixed}}$ is proportional to $(H/\sigma_{YS}^2)(\partial G/\partial a)|_{L\text{–fixed}}$. When the specimen geometry has an expression of energy release rate G, such that it is independent of crack length a under fixed-displacement, we can take $(\partial G/\partial a)|_{L\text{–fixed}} = 0$ and $(\partial r_y / \partial a)|_{L\text{–fixed}} = 0$. This seems very restrictive, but bimaterial specimens usually have a much longer crack length than other length parameters and have expressions for energy release rate which are nearly independent of crack length (Appendix C deals with the case where G is dependent on crack length). Since $(\partial r_y / \partial a)|_{L\text{–fixed}} = 0$, we can write $(\partial a_p / \partial a)|_{L\text{–fixed}}$ as

$$(\partial a_p / \partial a)|_{L\text{–fixed}} = r_y(\partial \eta / \partial a)|_{L\text{–fixed}}. \tag{B.8}$$

The plastic zone correction factor, η, is a function of many parameters such as elastic moduli, plastic properties, crack extension, etc, but all parameters except crack extension are constants during infinitesimal crack advance. Since η is not singular at $a = a_0$, where a_0 is the initial crack length before the crack growth, we can write $(\partial \eta / \partial a)$ in the Taylor series form as

$$(\partial \eta / \partial a)|_{L\text{–fixed}} = C_1 + C_2(a - a_0) + C_3(a - a_0)^2 + \cdots. \tag{B.9}$$

As can be seen in this equation, the interfacial toughness is dependent on the crack growth length, $a - a_0$. We measure the *R*-curve characteristics of materials in this point of view. However, further simplification can be made in the case of initiation toughness and steady state toughness. When we try to measure the initiation toughness at $a = a_0$, we can simply represent $(\partial \eta / \partial a)|_{L\text{–fixed}}$ and $(\partial a_p / \partial a)|_{L\text{–fixed}}$ as

$$(\partial \eta / \partial a)|_{L\text{–fixed},a=a_0} = C_1, \tag{B.10a}$$

$$(\partial a_p / \partial a)|_{L\text{–fixed},a=a_0} = C_1 r_y. \tag{B.10b}$$

We can also exploit Eqs. (B.10a) and (B.10b) to model the steady state toughness since the steady state toughness is independent of the crack growth length $a - a_0$ (i.e. $C_2 = C_3 = \cdots = 0$). If one tries to model the *R*-curve characteristics of the interfacial fracture, higher order terms of Eq. (B.9) must be taken into account. Using Eqs. (B.5), (B.10a) and (B.10b), it is found that the plastic dissipation is proportional to the plastic zone length r_y under the pre-mentioned conditions as

$$E_{\text{plastic}} = 4\gamma_{12}C_1 r_y \Delta a. \tag{B.11}$$

The total dissipation energy is given by

$$E_{\text{total}} = 2\gamma_{12}\{1 + 2C_1 r_y\}\Delta a. \tag{B.12}$$

Appendix C. Estimating the plastic dissipation energy for general specimen geometries

As in Appendix A, the plastic zone correction length a_p is given by

$$a_p = \eta r_y. \tag{C.1}$$

In order to calculate the plastic dissipation during interfacial crack growth, the change of a_p must be estimated as described in Section 2 and Appendix B. The plastic zone size r_y can be estimated via the elastic approximation as

$$r_y = \rho(\psi) \frac{GH}{\sigma_{\mathrm{YS}}^2}, \tag{C.2}$$

where ψ is measured with the characteristic length $h = \lambda K^2/\sigma_{\mathrm{YS}}^2$. The partial derivative of a_{p} with respect to the crack length a is written by

$$\frac{\partial a_{\mathrm{p}}}{\partial a} = \frac{\partial \eta}{\partial a} r_y + \eta \frac{\partial r_y}{\partial a} = \left(\frac{\partial \eta}{\partial a} + \eta \frac{1}{G} \frac{\partial G}{\partial a} \right) r_y(\psi). \tag{C.3}$$

Here, we consider more general specimen geometries than that presented in Section 2 and Appendix B. Since η and G are analytic at $a = a_0$, the series expansions of η and G at $a = a_0$ can be written as

$$\begin{aligned}
\eta &= C_0 + C_1(a - a_0) + C_2(a - a_0)^2 + \cdots, \\
G &= D_0 + D_1(a - a_0) + D_2(a - a_0)^2 + \cdots.
\end{aligned} \tag{C.4}$$

Then we can write $(\partial \eta/\partial a + \eta(1/G)\partial G/\partial a)$ as

$$\left(\frac{\partial \eta}{\partial a} + \eta \frac{1}{G} \frac{\partial G}{\partial a} \right) = A_0 + A_1(a - a_0) + A_2(a - a_0)^2 + \cdots. \tag{C.5}$$

When the initiation toughness of the interfacial crack is measured at $a = a_0$, we can simply represent $(\partial \eta/\partial a + \eta(1/G)\partial G/\partial a)$ as

$$\left. \left(\frac{\partial \eta}{\partial a} + \eta \frac{1}{G} \frac{\partial G}{\partial a} \right) \right|_{a=a_0} = A_0^{\mathrm{init}}. \tag{C.6}$$

We can estimate the plastic dissipation energy as

$$E_{\mathrm{plastic}} = 4\gamma_{12} \left(\frac{\partial a_{\mathrm{p}}}{\partial a} \right) \Delta a = 4\gamma_{12} A_0^{\mathrm{init}} r_y \Delta a. \tag{C.7}$$

When the steady state toughness is measured, the plastic dissipation is independent of the crack length a. We can write Eq. (C.5) as

$$\left(\frac{\partial \eta}{\partial a} + \eta \frac{1}{G} \frac{\partial G}{\partial a} \right) = A_0^{\mathrm{ss}}, \tag{C.8}$$

and the plastic dissipation energy for steady state cracking is written by

$$E_{\mathrm{plastic}} = 4\gamma_{12} \left(\frac{\partial a_{\mathrm{p}}}{\partial a} \right) \Delta a = 4\gamma_{12} A_0^{\mathrm{ss}} r_y \Delta a. \tag{C.9}$$

We obtain the relationships between the plastic dissipation and plastic zone size as Eqs. (C.7) and (C.9) for general specimen geometries and these relationships show that the plastic dissipation is proportional to the plastic zone size ahead of the interfacial crack tip. Eq. (C.7) or (C.9) has the same form with Eq. (B.11) or (2). It is noted that we assume that A_0^{init} and A_0^{ss} are independent of ψ. This assumption is justified by the comparison with Tvergaard and Hutchinson's [18] numerical results as presented in Section 6. The linear scaling of plastic zone length well represents their results (note that their numerical results are obtained without any assumption on specimen geometry).

References

[1] Cho YJ, Beom HG, Earmme YY. Application of a conservation integral to an interface crack interacting with singularities. Int J Fract 1994;65:63–73.

[2] Williams ML. The stresses around a fault or crack in dissimilar media. Bull Seismol Soc Am 1959;49:199–204.
[3] Rice JR, Sih GC. Plane problems of cracks in dissimilar media. J Appl Mech 1965;32:418–23.
[4] Park JH, Earmme YY. Application of conservation integrals to interfacial crack problems. Mech Mater 1986;5:261–76.
[5] Hutchinson JW, Suo Z. Mixed mode cracking in layered materials. In: Hutchinson JW, Wu TY, editors. Advances in applied mechanics, vol. 29. New York: Academic Press; 1991. p. 191.
[6] Shih CF, Asaro RJ. Elastic–plastic analysis of cracks on bimaterial interfaces: Part I—small scale yielding. J Appl Mech 1988;55:299–316.
[7] Shih CF, Asaro RJ. Elastic–plastic analysis of cracks on bimaterial interfaces: Part II—structure of small-scale yielding fields. J Appl Mech 1989;56:763–79.
[8] Zywicz E, Parks DM. Small-scale yielding interfacial crack-tip fields. J Mech Phys Solids 1992;40:511–36.
[9] Chiang MYM, Chai H. Plastic deformation analysis of cracked adhesive bonds loaded in shear. Int J Solids Struct 1994;31:2477–90.
[10] Chiang MYM, Chai H. Finite element analysis of interfacial crack propagation based on local shear, Part I—near tip deformation. Int J Solids Struct 1998;35:799–813.
[11] Cao HC, Evans AG. An experimental study of the fracture resistance of bimaterial interfaces. Mech Mater 1989;7:295–304.
[12] Thouless MD. Fracture of a model interface under mixed-mode loading. Acta Metall Mater 1990;38:1135–40.
[13] Wang J-S, Suo Z. Experimental determination of interfacial toughness curves using Brazil-nut-sandwiches. Acta Metall Mater 1990;38:1279–90.
[14] Liechti KM, Chai YS. Asymmetric shielding in interfacial fracture under in-plane shear. J Appl Mech 1992;59:295–304.
[15] Liang Y-M, Liechti KM. Toughening mechanisms in mixed-mode interfacial fracture. Int J Solids Struct 1995;32:957–78.
[16] Chai H. Micromechanics of shear deformations in cracked bounded joints. Int J Fract 1992;58:223–39.
[17] Chai H. Deformation and failure of adhesive bonds under shear loading. J Mater Sci 1993;28:494–506.
[18] Tvergaard V, Hutchinson JW. The influence of plasticity on mixed mode interface toughness. J Mech Phys Solids 1993;41:1119–35.
[19] Needleman A. A continuum model for void nucleation by inclusion debonding. J Appl Mech 1987;54:525–31.
[20] Yang QD, Thouless MD, Ward SM. Elastic–plastic mode-II fracture of adhesive joints. Int J Solids Struct 2001;38:3251–62.
[21] Evans AG, Hutchinson JW, Wei Y. Interface adhesion: effects of plasticity and segregation. Acta Mater 1999;47:4093–113.
[22] Hutchinson JW, Evans AG. Mechanics of materials: top-down approaches to fracture. Acta Mater 2000;48:125–35.
[23] Shivakumar KN, Crews Jr JH. Energy dissipation associated with crack extension in an elastic–plastic material. Eng Fract Mech 1987;28:319–30.
[24] Zywicz E, Parks DM. Elastic yield zone around an interfacial crack tip. J Appl Mech 1989;56:577–84.
[25] Rice JR, Suo Z, Wang JS. Mechanics and thermodynamics of brittle interface failure in bimaterial systems. In: Ruhle M, Evans AG, Ashby MF, Hirth JP, editors. Metal–ceramic interfaces. Oxford: Pergamon Press; 1990. p. 269–94.
[26] Rice JR. Elastic fracture mechanics concepts for interfacial cracks. J Appl Mech 1988;55:98–103.
[27] Banks-sills L, Ashkenazi D. A note on fracture criteria for interface fracture. Int J Fract 2000;103:177–88.
[28] Charalambides M, Kinloch AJ, Wang Y, Williams JG. On the analysis of mixed-mode failure. Int J Fract 1992;54:269–91.
[29] Rice JR. Limitations to the small scale yielding approximation for crack tip plasticity. J Mech Phys Solids 1974;22:17–26.
[30] Hauf DE, Parks DM, Lee H. A modified effective crack-length formulation in elastic–plastic fracture mechanics. Mech Mater 1995;20:273–89.